Structural and optical characteristics of Er-doped SRSO layers deposited by the confocal sputtering technique

K. Hijazi, L. Khomenkova, J. Cardin, F. Gourbilleau *, R. Rizk

CIMAP, UMR CNRS/CEA/ENSICAEN/Université de Caen, 6 Bd. Marechal Juin, 14050 Caen Cedex, France

ABSTRACT

Er-doped silicon-rich silicon oxide layers have been grown at 600 °C by magnetron co-sputtering of three confocal cathodes (Si, SiO_2 and Er_2O_3) in pure argon plasma. The structural and optical properties of the layers were examined in the function of deposition and annealing conditions. It was shown that the increase of the RF power density applied on the Si cathode from 0.74 to 2.07 W cm^{-2}, while maintaining constant RF power on the two other cathodes, allows a fine engineering of the Si excess from 5 to 15 at%. The Er content was evaluated to 1×10^{21} at cm^{-3}. A high Er^{3+} emission was observed under non-resonant (476 nm) excitation from as-deposited layers, which was significantly improved after annealing at 600 °C. The Er PL was found to be much more intense than the best samples reported so far, which was annealed at 900 °C and contains, however, lower Er content (5.4×10^{20} at cm^{-3}) and Si excess (7 at% of Si). The Er emission lifetime was found to be about 6 ms for low Si excess (5 at%) and 1–2 ms for high Si excess. Upon reducing the Er content by a factor of three, the Er^{3+} PL intensity was further increased and the lifetime reached 5.5 ms, suggesting a notable increase of the fraction of coupled Er ions.

1. Introduction

The emission at 1.54 μm related to the $^4I_{13/2} \rightarrow {}^4I_{15/2}$ internal transitions of Er ions plays an important role in the development of telecommunications, because of its minimum absorption by silica, which is widely used in Er-doped fiber amplifiers [1]. However, Er-doped silica suffers from two limitations: a low excitation cross-section of Er ($\sim 5 \times 10^{-21}$ cm^2 at 1.54 μm) [2] and a low solubility that induces Er clustering with the concentration-related detrimental effects [3]. To improve both Er excitation and device packaging, a great effort has been devoted since several years to benefit from the broad-band high-absorbing Si nanoclusters (Si-nc) as sensitizers of the neighboring Er ions in silicon-rich silicon oxide (SRSO) [4–7]. This allows the enhancement of the effective excitation of Er ions by 3–4 orders of magnitude and the use of high-power LEDs or electrical excitation instead of the expensive pump lasers. Such an approach seems promising for the development of compact Er-doped waveguide amplifiers (EDWAs). The achievement of a net gain in EDWAs has been thwarted so far by two main difficulties: the reduction of the carrier absorption found responsible for the main losses [8] and the necessity of enhancing the low number of Er coupled to Si-nc

estimated recently to a few % [9,10]. To overcome these issues, a careful engineering of both composition and morphology of the material is necessary to grow very small Si-nc with high density. Their smallness is expected to minimize the confined carrier absorption effect [11], while their high density is liable to couple an optimum concentration of Er ions.

This paper deals with a novel approach for our team aiming at allowing the optimization of Si excess for the growth of appropriate Si-nc density that ensures the coupling with maximum Er ions.

2. Experiment

The Er-SRSO layers were grown by the magnetron co-sputtering of three cathodes, namely SiO_2, Si and Er_2O_3, under a plasma of pure argon maintained at a pressure of 3 mTorr. The RF power density applied on the Si cathode (P_{Si}^{RF}) was changed from 0.74 to 2.07 W cm^{-2} to vary the Si excess incorporated, while for the SiO_2 and Er_2O_3 targets they were fixed at 7.4 and 0.74 W cm^{-2}, respectively. The depositions were made at $T_S = 600$ °C on a rotating substrate, hence ensuring good homogeneity of both composition and thickness. The latter was in the range 1–1.5 μm. The deposited films were subsequently annealed under a nitrogen flux, for 1 h at different temperatures, T_a, between 600 and 800 °C. To investigate the structural and configurational properties,

Fourier transform infrared (FTIR) spectra were recorded under Brewster incident (65°), using a Nicolet Nexus spectrometer. Energy dispersive X-ray spectroscopy (EDX) was used to determine the Er content, which was found close to 10^{21} cm^{-3} for all samples. The refractive index and thickness of the layers were obtained by M-lines measurements performed in reflection configuration [12–14]. These measurements were made by means of a He–Ne laser operating at 632.8 nm (1.95 eV) polarized in the transverse electric (TE) mode. The optical properties were examined by PL measurements using two excitation lines, the resonant 488 nm and non-resonant 476 nm delivered by an Ar$^+$ laser. The pumping at 476 nm was used to ensure that Er emission was stimulated by the energy transfer from the Si-nc sensitizers. The Er PL was measured with a Jobin Yvon 1 m single grating monochromator and Northcoast Germanium detector cooled with liquid nitrogen. The PL signal was recorded through an SRS lock-in amplifier (SP830 DPS) referenced to the chopping frequency of light of 20 Hz. The time-resolved Er PL was measured with the already-described PL system, the signal being displayed by a Tektronix oscilloscope (TDS 3012B).

3. Results and discussion

Fig. 1 shows the FTIR spectra recorded on the samples deposited at 600 °C with different P_{Si}^{RF} values before being annealed at 600 °C. The FTIR spectrum corresponding to the layer prepared at $P_{Si}^{RF} = 0$ with the same conditions but free from Si excess, i.e. silica film deposited at 600 °C, is also shown for comparison. All the spectra were acquired at Brewster incident to avoid any reflection and detect the longitudinal optical (LO$_3$) mode associated with the Si/SiO$_2$ interface at 1250 cm^{-1} [15], and then normalized with respect to the transversal optic (TO$_3$) mode at about 1080 cm^{-1}. By increasing the P_{Si}^{RF} value, one notices a gradual merging of the doublet TO$_4$–LO$_4$ located around 1160–1200 cm^{-1}, which occurs apparently at the expense of the LO$_3$ peak, which shows a progressive decrease. Such a merging reflects some increase of the disorder [16] that can be merely attributed to the increasing amount of the Si excess, expected to take place when P_{Si}^{RF} is increased. It is worth noting that the evolution of the LO$_3$ mode is much more governed by the disorder than by the behavior of the Si/SiO$_2$ interface, since the annealing

temperature (600 °C) is too low to grow Si-nc but might induce the formation of some 'atomic' scale sensitizers [17]. The 'usual' Si-nc sensitizers are rather grown at much higher temperatures in such a material [17,18], giving rise to a signature of the Si/SiO$_2$ interface, as shown by the FTIR spectrum reported in the inset for a sample containing 14 at% of Si excess and annealed at 1100 °C. Indeed, the signature of the Si/SiO$_2$ interface appears more pronounced than that for the case of annealing at 600 °C, and then attest the formation of Si-nc, even though the high level of LO$_4$–TO$_4$ still reflects the important disorder of the host matrix attributed to the high values of both Si excess and Er content. To better correlate this power P_{Si}^{RF} density to the Si excess, we have proceeded to a rough estimate of their amount in substoichiometric SiO$_x$ from the FTIR spectra by the method described in Ref. [19]. One can observe a gradual increase of the Si excess from about 5 to about 15 at% when the P_{Si}^{RF} density increases from 0.74 to 2.07 W cm^{-2} (Fig. 2). Such an evolution was also confirmed for other series of samples obtained with different T_S values (not shown here).

The progressive increase of the Si excess with the power density is also reflected by the concomitant evolution of the refractive index n, as determined by M-lines measurements. Indeed, n increases with the Si excess, which was roughly estimated by the FTIR-based approach, as already specified.

Concerning the emission properties, Fig. 3 compares the evolution of the PL intensity at 1.54 μm as a function of the photon flux of a non-resonant line (476 nm), for three samples: the reference sample (R) obtained using the previous method consisting the reactive sputtering of a single SiO$_2$ cathode topped by Er$_2$O$_3$ chips, as previously described [11,18,20], and the as-deposited and annealed samples obtained by the magnetron co-sputtering of three confocal cathodes, described above. The reference R contains 7 at% Si and 5.4×10^{20} Er cm^{-3} and was annealed at 900 °C during 10 min, while the present samples contain 10 at% Si and 1×10^{21} Er cm^{-3} with one annealed at only 600 °C during 1 h. It is important to note that the PL intensity increases for the three samples when the photon flux is increased between 2×10^{18} and 7×10^{19} ph cm^{-2} s^{-1}. In this flux range, the impact of the up-conversion process on our annealed sample, which shows a quasi-linear increase, is much weaker than that on the reference sample, and can be therefore considered as a non-limiting factor. Anyway, all along the flux range, the PL intensity of the as-deposited sample is higher than that for the R layer, and this PL emission is further improved for the sample annealed at a temperature as low as 600 °C. The inset compares the PL spectra
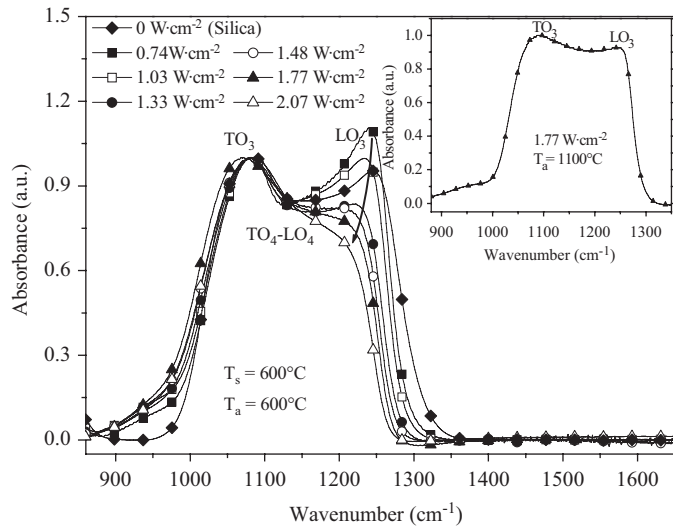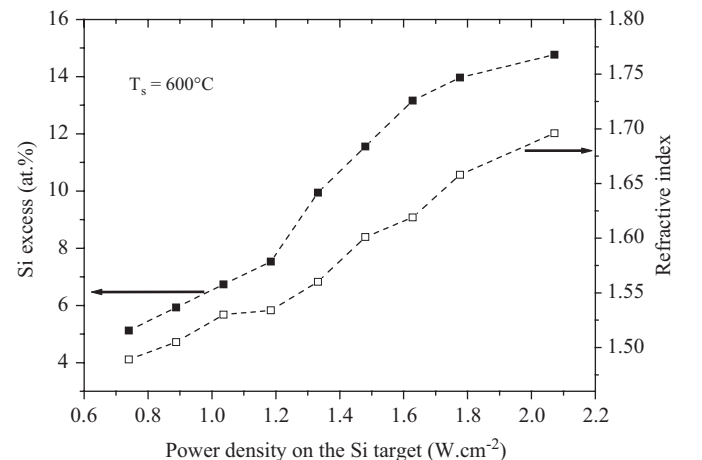

Fig. 1. FTIR spectra of the samples annealed at 600 °C and previously deposited at 600 °C with the indicated values of the power density applied on the Si target. The inset shows the FTIR spectrum for the sample deposited with P_{Si}^{RF} density = 1.77 W cm^{-2} and annealed at 1100 °C.

Fig. 2. Variation of the Si excess, as estimated from the FTIR spectra, and evolution of the refractive index obtained by M-lines measurements, in function of the power density applied on the Si target.
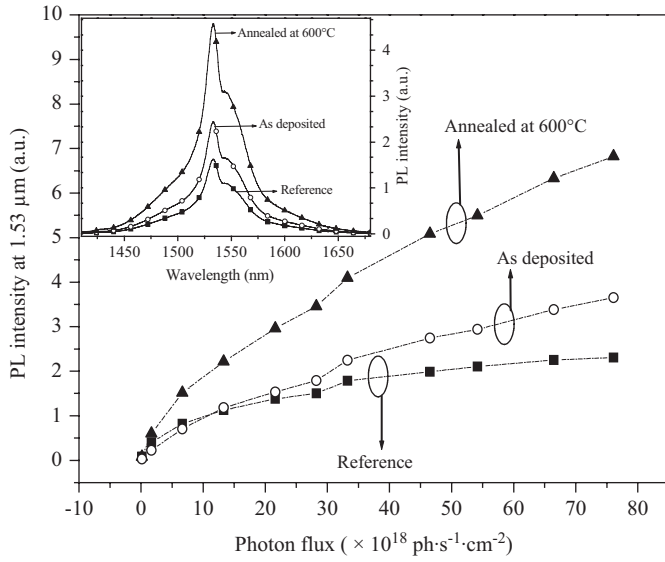
Fig. 3. Comparison of the PL intensity at $1.54\,\mu m$ recorded with a non-resonant (476 nm) line on the reference sample (R) (see text) and on the present samples: as-deposited and annealed at $600\,°C$. The inset reports the PL spectra for the reference sample (R) and the two as-deposited and annealed (at $600\,°C$) samples for a photon flux of about $6 \times 10^{19}\,ph\,cm^{-2}\,s^{-1}$.

obtained on the as-deposited and annealed (at $600\,°C$) samples to that of the reference sample (R), under a non-resonant 476 nm excitation line with a flux of about $6 \times 10^{19}\,ph\,cm^{-2}\,s^{-1}$. It is worth noting that the 1.53-μm PL intensity from the as-deposited sample is nearly 1.5 times higher than that from the R layer. This PL emission was further improved by a factor ~ 3 after annealing at $600\,°C$. The detection of PL from the as-deposited layer, never or rarely observed from as-grown samples, is likely due to the high deposition temperature ($600\,°C$), which seems to favor, during the growth, the formation of some sensitizers, which could be compared to the already mentioned 'atomic' scaled sensitizers described in Ref. [17]. Nevertheless, due to their poor contrast and their small size, such agglomerates have not been successfully evidenced by high-resolution electron microscopy [17]. The annealing at $600\,°C$ allows the recovery of non-radiative defects and/or the relaxation of the matrix network, leading to some improvement of Er PL.

Fig. 4(a) shows the evolution of the PL intensity at $1.54\,\mu m$ for the indicated annealing temperatures as a function of Si excess estimated from the analysis of FTIR spectra. During the first stages of increase of Si excess, the Er PL shows a gradual improvement for the as-deposited and all annealed samples, up to a maximum corresponding to about 10 at% of Si excess, before decreasing for higher values of Si excess. The highest PL is shown by the samples annealed at $600\,°C$, all over the range of Si excess, hence generalizing the performance of that similarly annealed and enriched with 10 at% of Si, as displayed in Fig. 3. This observation supports our earlier suggestion of the occurrence of the highest Er–Si-nc coupling for $T_a = 600\,°C$. The same explanation can still be valid for the evolution of the PL shown in Fig. 4(a). For a constant concentration of Er, the coupled fraction is expected to increase with the Si excess, up to an optimum value corresponding to a maximum density of sensitizers Si-nc growing/aggregating on the seeds available in a given sample. When the value of Si excess exceeds a given value, one expects some saturation of the available seeds, leading to an increase of the average size of the Si-nc at the expense of their efficiency as sensitizers and/or their density in case of coalescence. Anyway, beyond a given value, the impact of Si excess becomes detrimental to the quality of the
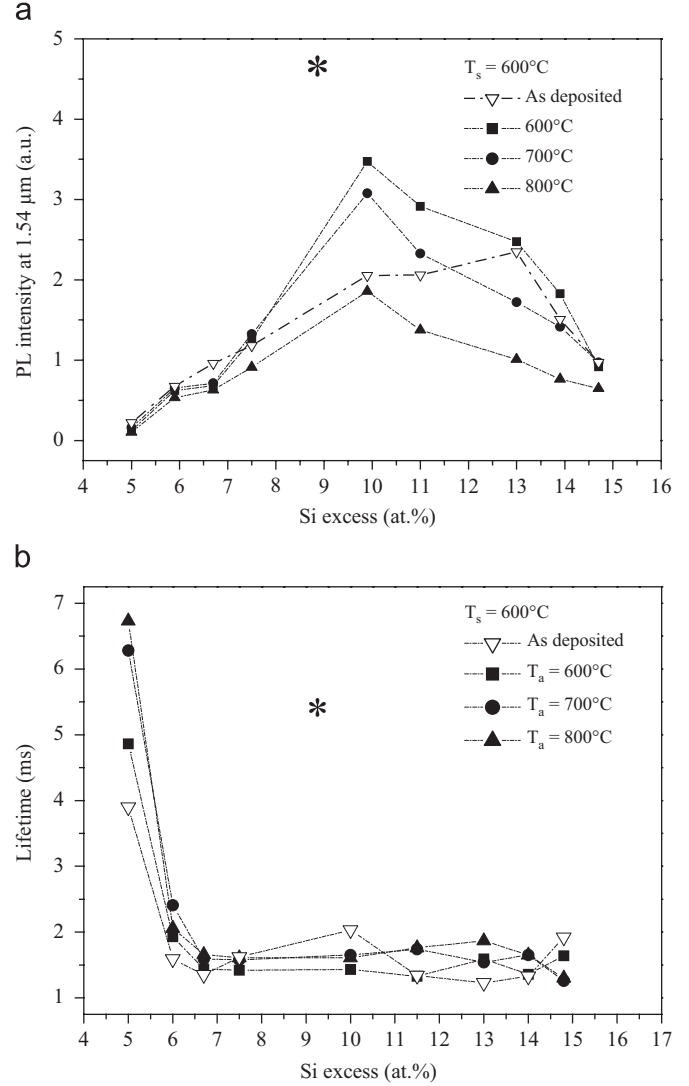

Fig. 4. (a): The PL intensity at $1.54\,\mu m$ as a function of the Si excess with non-resonant excitation ($\lambda = 476$ nm), for the as-deposited and annealed samples at the indicated temperature. (b): Evolution of the emission lifetime for the samples of Fig. 4(a) against the Si excess. The two experimental points labeled by (*) for the PL intensity and lifetime were obtained for the sample containing lower Er content than those of the main plots (3.5×10^{20} vs. 10^{21} at cm^{-3}) and a Si excess of about 9 at%.

matrix, as confirmed by the evolution of the doublet TO$_4$–LO$_4$. (Fig. 1). Concerning the emission properties, the lifetime shows a dramatic deterioration from a value higher than 6 ms for a Si excess of about 5 at% to 1–2 ms when the Si excess is higher than 7 at%, as displayed in Fig. 4(b). Nevertheless, one has to note that the Er concentration of 10^{21} at cm^{-3} is relatively high compared to that for the R sample and could also be one of the reasons for the observed improvement in the PL intensity. Moreover, such a high concentration is expected to generate, for high fluxes, cooperation up-conversion phenomena and other concentration quenchings, which are also harmful for both coupling/emission efficiency and lifetime. To counter these, a series of samples have been lately prepared with 3.5×10^{20} Er cm^{-3}. A typical preliminary result is reported for a sample containing also an optimum Si excess (~ 9 at%). The corresponding data for the Er PL intensity and emission lifetime are labeled by stars in Fig. 4(a) and (b). One can notice that, in addition to some 25% improvement of the Er PL, the emission lifetime has been significantly increased from 1 to 2 ms for the present samples to about 5.5 ms for those under studies.

Since this sample contains an Er content comparable to that for the reference layer, the observed improvement of its PL intensity reflects in all likelihood a consequent increase in the fraction of coupled Er ions. Anyway, the work is in progress for further optimization of both Si excess and Er content.

4. Conclusion

In conclusion, we have fabricated a series of samples with different Si excess by magnetron co-sputtering of three confocal cathodes that were subsequently characterized by different techniques. Both as-deposited (at 600 °C) and annealed samples showed Er PL intensity much higher compared to the 'standard' sample previously described in Refs. [10,11]. The maximum Er PL was obtained for the sample annealed at 600 °C for 1 h and containing 10 at% of Si excess with a lifetime of 1–2 ms. By reducing the disadvantageous high Er content ($\sim 10^{21}$ at cm^{-3}) responsible fro detrimental concentration-related effects, by a factor of three, the PL intensity was further improved and the lifetime enhanced to about 5.5 ms. This might suggest an increasing proportion of the Er ions coupled to Si-nc.

Acknowledgment

References

[1] E. Desurvire, J.R. Simpson, P.C. Pecker, Opt. Lett. 12 (1987) 888.
[2] J. Miniscalco, J. Lightwave Technol. 9 (1991) 234.
[3] A. Polman, J. Appl. Phys. 82 (1997) 1.
[4] A.J. Kenyon, P.F. Trwoga, M. Federighi, C.W. Pitt, J. Phys. 6 (1994) L319.
[5] M. Fujii, M. Yoshida, Y. Kanzawa, S. Hayashi, K. Yamamoto, Appl. Phys. Lett. 71 (1997) 1198.
[6] H. Przybylinska, W. Jantsch, Yu. Suprun-Belevitch, M. Stepikhova, L. Palmetshofer, G. Hendorfer, A. Kozanecki, Phys. Rev. B 54 (1996) 2532.
[7] G. Franzò, V. Vinciguerra, F. Priolo, Appl. Phys. A: Mater. Sci. Process 69 (1999) 3.
[8] N. Daldosso, D. Navarro-Urrios, M. Melchiorri, L. Pavesi, F. Gourbilleau, M. Carrada, R. Rizk, C. Garcia, P. Pellegrino, B. Garrido, L. Cognolato, Appl. Phys. Lett. 86 (2005) 261103.
[9] M. Wojdak, M. Klik, M. Forcales, O.B. Gusev, T. Gregorkiewicz, D. Pacifici, G. Franzò, F. Priolo, F. Iacona, Phys. Rev. Lett. 69 (2004) 233315.
[10] B. Garrido, C. García, S.-Y. Seo, P. Pellegrino, D. Navarro-Urrios, N. Daldosso, L. Pavesi, F. Gourbilleau, R. Rizk, Phys. Rev. B 76 (2007) 245308.
[11] N. Daldosso, D. Navarro-Urrios, M. Melchiorri, C. Garcia, P. Pellegrino, B. Garrido, C. Sada, G. Battaglin, F. Gourbilleau, R. Rizk, L. Pavesi, IEEE J. Sel. Top. Quantum Electron. 12 (2006) 1607.
[12] R.T.H. Kersten, J. Mod. Opt. 22 (1975) 503.
[13] R. Ulrich, R. Torge, Appl. Opt. 12 (1973) 2901.
[14] J. Cardin, D. Leduc, Appl. Opt. 47 (2008) 894.
[15] J.E. Olsen, F. Shimura, J. Appl. Phys. 66 (1989) 1353.
[16] T. Kirk, Phys. Rev. B 38 (1988) 1255.
[17] O. Savchyn, F.R. Ruhge, P.G. Kik, R.M. Todi, K.R. Coffey, H. Nukala, H. Heinrich, Phys. Rev. B 76 (2007) 195419.
[18] F. Gourbilleau, C. Dufour, M. Levalois, J. Vicens, R. Rizk, C. Sada, F. Enrichi, G. Battaglin, J. Appl. Phys. 94 (2003) 3896.
[19] F. Yun, B.J. Hinds, S. Hatatani, S. Oda, Q.X. Zhao, M. Willander, Thin Solid Films 375 (2000) 137.
[20] F. Gourbilleau, M. Levalois, C. Dufour, J. Vicens, R. Rizk, J. Appl. Phys. 95 (2004) 3717.